Eur. Phys. J. B **33**, 215–219 (2003)
DOI: 10.1140/epjb/e2003-00159-6

THE EUROPEAN PHYSICAL JOURNAL B

Coherent transport through intramolecular junction of single-wall carbon nanotubes

L. Yang[a], J. Chen, H. Yang, and J. Dong

Group of Computational Condensed Matter Physics, National Laboratory of Solid State Microstructures and Department of Physics, Nanjing University, Nanjing 210093, PR China

Received 14 January 2003 / Received in final form 25 February 2003
Published online 4 June 2003 –

Abstract. We have constructed four types single-wall carbon nanotube intramolecular junctions (IMJs) of (5,5)/(8,0), (5,5)/(10,0), (5,5)/(9,0)**A**, and (5,5)/(9,0)**B** along a common axis, and calculated their electronic and transport properties using a tight binding-based Green's function approach that is particular suitable for realistic calculation of electronic transport property in extended system. Our results show that quasi-localized states can appear in the metal/semiconductor heterojunctions ((5,5)/(8,0) and (5,5)/(10,0)junctions), which is desirable for the design of a quantum device; and the conductance of M-M IMJs is very sensitive to the connectivity of the matching tubes, certain configurations of connection completely stop the flow of electron, while others permit the transmission of the current through the interface. These results may have implications for the device assembly and manipulation process of all carbon nanotubes-based microelectronic elements.

PACS. 71.15.Dx Computational methodology (Brillouin zone sampling, iterative diagonalization, pseudopotential construction) – 73.20.At Surface states, band structure, electron density of states – 73.40.-c Electronic transport in interface structures – 81.07.De Nanotubes

The rapid miniaturization of electronics to the micrometer-scale has been a key force driving scientific and economic progress over the past 25 years. Nanometer-scale electronics (nanoelectronics) is the closely watched next frontier [1]. The anticipated limits to the further miniaturization have led to intense research directed toward the development of molecular electronics. The use of single-wall carbon nanotubes (SWNTs) has stimulated these efforts because these molecules exhibit a range of suitable properties, depending on their diameter and chirality, SWNTs can be either one dimensional metals or semiconductors. Various basic components have been demonstrated, such as molecular wires, switches, and diodes [2,3]. Bachtold *et al.* find that individual semiconducting SWNT adsorbed between two metal contacts on a silicon substrate behaves like the field-effect transistors in today's microcomputers, and several nanotube devices integrated onto a chip demonstrate digital logic operation [2,4,5]. Much smaller devices could be made by joining two nanotubes or nanowires to create, for examples, metal-semiconductor junctions, in which the junction area would be about 1 nm^2 for SWNTs. Until now, one of the major challenges facing molecular electronics was the assembly of individual molecules or molecular-scale structures into functioning logic circuits. So, it is especially necessary to study the transport property through intramolecular junction of carbon nanotubes.

The structure and properties of a defect-free SWNT are completely determined by the circumferential vector $\boldsymbol{c}_h = n_1\boldsymbol{a}_1 + n_2\boldsymbol{a}_2 \equiv (n_1, n_2)$ that connects crystallographically equivalent sites on a two-dimensional graphene sheet, where $\boldsymbol{a}_1$ and $\boldsymbol{a}_2$ are the graphene lattice vectors and n_1 and n_2 are integers. The introduction of topological defects in the hexagonal bond network of a nanotube changes its chirality and therefore its electronic characters. The defects must induce zero net curvature to prevent the tube from flaring or closing. Minimal local curvature is desirable to minimize the defect energy. The smallest topological defect with minimal local curvature and zero net curvature is a pentagon-heptagon pair. On-tube junction formed from the topological defect that connects two nanotubes of different chirality in a seamless way. Since nanotubes are metallic (M) or semiconducting (S), such a topological defect defined an molecular-size M-M, M-S, or S-S heterojunctions may show unique quasi-one-dimensional transport properties [6–9], thereby opening up the intriguing possibility of forming all-carbon nanotube-based microelectronics [1–4]. Some of these remarkable theoretical predictions have been confirmed by scanning tunnelling microscopy (STM) and scanning tunnelling spectroscopy (STS) experiments [10–12].

Single-walled carbon nanotubes (SWNTs) intramolecular junctions (IMJs) are formed by interposing one or

[a] e-mail: lfyzz@yahoo.com.cn

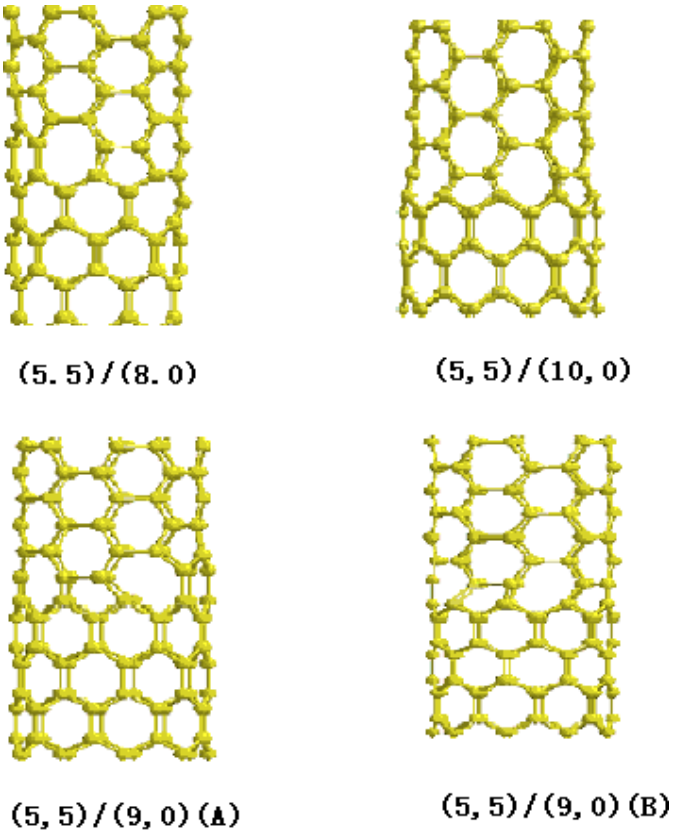

Fig. 1. Atomic structures of (5,5)/(8,0), (5,5)/(10,0), (5,5)/(9,0)**A**, (5,5)/(9,0)**B** SWNT IMJs.

multiple topological pentagon-heptagon (5-7) defects (in the normal hexagonal structure) between two nanotube segments of different helicity. Experiments have shown that IMJs are present in SWNT samples and topological defects occur with a relatively high frequency in the samples grown by laser ablation [12]. To study the electronic properties of IMJs and transport properties through IMJs, we have constructed four types SWNT IMJ of (5,5)/(8,0), (5,5)/(10,0), (5,5)/(9,0)**A**, and (5,5)/(9,0)**B** along a common axis as seen in Figure 1 where (5,5)/(8,0) and (5,5)/(10,0) are metal/semiconductor IMJs, (5,5)/(9,0)**A** and (5,5)/(9,0) **B** are metal/metal IMJs, **A** and **B** denote two different configuration of 5-7 defects on the (5,5)/(9,0) IMJs. The pentagon-heptagon pairs and their connections mode to other hexagon bond net can be clearly seen from a two-dimensional map of the IMJ structures (Fig. 2). All the four IMJ structures are optimized using CFF95 force field in Cerius2 program package and proved to be stable.

We describe the carbon nanotubes system by a tight-binding model with one π electron per atom. Our tight-binding Hamiltonian is of the form

$$H = -V_{pp\pi} \sum_{\langle ij \rangle} a_i^\dagger a_j + \text{c.c.}, \tag{1}$$

where the sum in i, j is restricted to nearest-neighbor, and $V_{pp\pi} = 2.66$ eV [6]. The other tight-binding terms are neglected in this approach. On-site energies are set to zero. Within this theory, graphite sheets and defect-free nanotubes have complete electron-hole symmetry with their Fermi levels at zero. For simplicity all nearest-neighbor hopping parameters are assumed to be equal, independent of the length, location, and orientation of the bonds on the matched tubes. Deviations in bond lengths due to reconstruction near the interface are neglected. Hence, we study the changes induced solely by the alterations in the topology of the hexagonal rolled lattice.

To investigate the electronic properties and quantum transport through IMJs of carbon nanotubes, we have used the tight-binding Green's function-based approach [13,14]. This approach is particularly suitable for realistic calculation of electronic transport property in extended systems to a general configuration of a left-lead/conductor/ right-lead (L-C-R). The method allows us to fully consider the complete of the semi-infinite leads with a very limited computational cost. Moreover, the only quantities that enter into the present formulation are the matrix elements of the Hamiltonian operator, with no need for the explicit knowledge of the electron wave functions for the multichannel expansion. In the present case, the leads are ideal nanotubes, and the conductor is represented by a defective or the distorted region (junction). A fundamental result in the theory of electronic transport is that the conductance through a region of interacting electrons (the C region) is related to the scattering properties of the region itself *via* the Landauer formula:

$$\mathcal{C} = \frac{2e^2}{h}\mathcal{T}, \tag{2}$$

where $\mathcal{T}$ is the transmission function and $\mathcal{C}$ is the conductance. the formula represents the probability that an electron injected at one end of the conductor will transmit to the other end. The transmission function can be expressed in terms of the Green's functions of the conductors and the coupling of the conductor to the leads [15,16]:

$$\mathcal{T} = \text{Tr}(\Gamma_L G_C^r \Gamma_R G_C^a), \tag{3}$$

where $G_C^{\{r,a\}}$ are the retarded and advanced Green's functions of the conductor, and $\Gamma_{\{L,R\}}$ are functions that describe the coupling of the conductor to the leads. The Green's function for the whole system can be explicitly written as

$$G_C = (\epsilon - H_C - \Sigma_L - \Sigma_R)^{-1}, \tag{4}$$

where we define $\Sigma_L = h_{LC}^\dagger g_L h_{LC}$ and $\Sigma_R = h_{RC} g_R h_{RC}^\dagger$ as the self-energy terms due to the semi-infinite leads, h_{LC} and h_{RC} are the coupling matrices that will be nonzero only for adjacent points in the conductor and leads, and $g_{\{L,R\}} = (\epsilon - H_{\{L,R\}})^{-1}$ are the leads' Green's functions. The self-energy terms can be viewed as effective Hamiltonian that arise from the coupling of the conductor with the leads. Once the Green's functions are known, the coupling functions $\Gamma_{\{L,R\}}$ can be easily obtained as [17]

$$\Gamma_{\{L,R\}} = \text{i}\left[\Sigma_{\{L,R\}}^r - \Sigma_{\{L,R\}}^a\right], \tag{5}$$

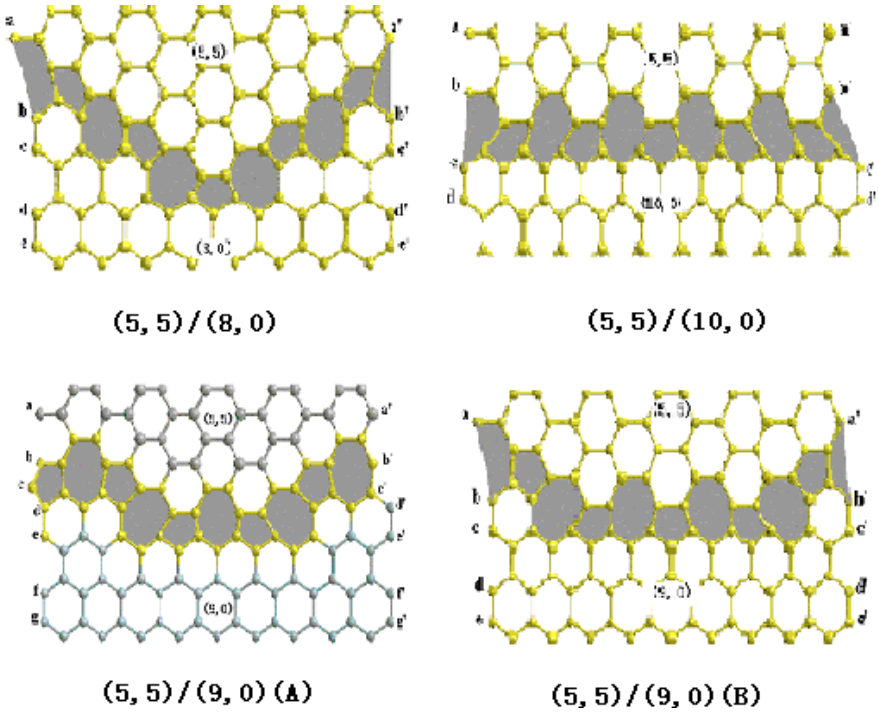

Fig. 2. Two-dimensional representations of (5,5)/(8,0), (5,5)/(10,0), (5,5)/(9,0)**A**, (5,5)/(9,0)**B** SWNT IMJs.

where the advanced self-energy $\Sigma^a_{\{L,R\}}$ is the Hermitian conjugate of the retarded self-energy $\Sigma^r_{\{L,R\}}$. The expression of the self-energies can be deduced along the lines of reference [11] using the formalism of principal layers in the framework of the surface Green's function matching theory [18]. We obtain

$$\begin{aligned}\Sigma_L &= H^\dagger_{LC}(\epsilon - H^L_{00} - (H^L_{01})^\dagger \overline{T}_L)^{-1} H_{LC}, \Sigma_R \\ &= H_{CR}(\epsilon - H^R_{00} - H^R_{01} T_R)^{-1} H^\dagger_{CR}, \end{aligned} \quad (6)$$

where $H^{L,R}_{nm}$ are the matrix elements of the Hamiltonian between the layer orbital of the left and right leads, respectively, and $T_{L,R}$ and $\overline{T}_{L,R}$ are the appropriate transfer matrices. The latter are easily computed from the Hamiltonian matrix elements *via* an iterative procedure [13,19]. Correspondingly, H_{LC} and H_{CR} are the coupling matrices between the conductor and the leads.

The knowledge of the bulk Green's function G also includes the electronic properties information of system, which can be used to calculate the density of states (DOS) and the local density of states (LDOS) *via* the spectral theorem of the bulk Green's function.

$$D(E) = -\frac{1}{\pi}\mathrm{Im}[\mathrm{Tr}G(E)], LD_n(E) = -\frac{1}{\pi}\mathrm{Im}[G_{n,n}(E)], \quad (7)$$

where $D(E)$ and $LD_n(E)$ are DOS and $LDOS$ with energy E, and n is the atom label. The Green's function(GF) of the complete structure is obtained from the bulk GFs of the constituent tubes and the interface Hamiltonian. Localized and extended states are directly obtained from the GF.

The electronic properties of the metal/semiconductor IMJs ((5,5)/(8,0) and (5,5)/(10,0) junctions) and metal/metal IMJs((5,5)/(9,0)**A** and (5,5)/(9,0)**B**) are illustrated in Figures 3 and 4. We averaged the LDOS over each interface region because quantum interference effects distort the LDOS on individual atomic sites. Figures 3 and 4 show the atom-averaged LDOS of M-S interface and M-M interface respectively, the LDOS of the constituents perfect tubes are also plotted for comparison. The Fermi energy ϵ_F coincides with the atomic π level, taken as zero of energy. The energies of the eigenstates are within $|E| \leq 3 \times V_{pp\pi}$, which is consistent with three C-C bonds from each carbon atom. The (5,5) and (9,0) tubes are metallic, with a nonzero density of states at ϵ_F. The LDOS of these tubes present a plateau indicating the existence of one-dimensional metallic energy bands. The (8,0) and (10,0) tubes are semiconducting with finite band gaps. Both isolated nanotube densities of states not only present the two-dimensional van Hove singularities of graphite at $E = \pm V_{pp\pi}(\pm 2.66$ eV), but also sharp peaks coming from the inverse square-root divergence $\frac{1}{\sqrt{E}}$ of the spectra of the one-dimensional (1D) bands. These singularities are due to the quantization of the 1D energy bands in the circumferential direction. By comparison with the interface LDOS, Figure 3 shows allowed states in the energy range of the gap of the perfect semiconducting component, these metal-induced gap states are characteristic of metal-semiconductor junctions. Figure 4 shows a slight enhancement of the LDOS in the energy range around the Fermi energy ϵ_F although the conductance is suppressed in this region. Of special interest in the electronic states of these systems are the emergence of sharp peaks in the

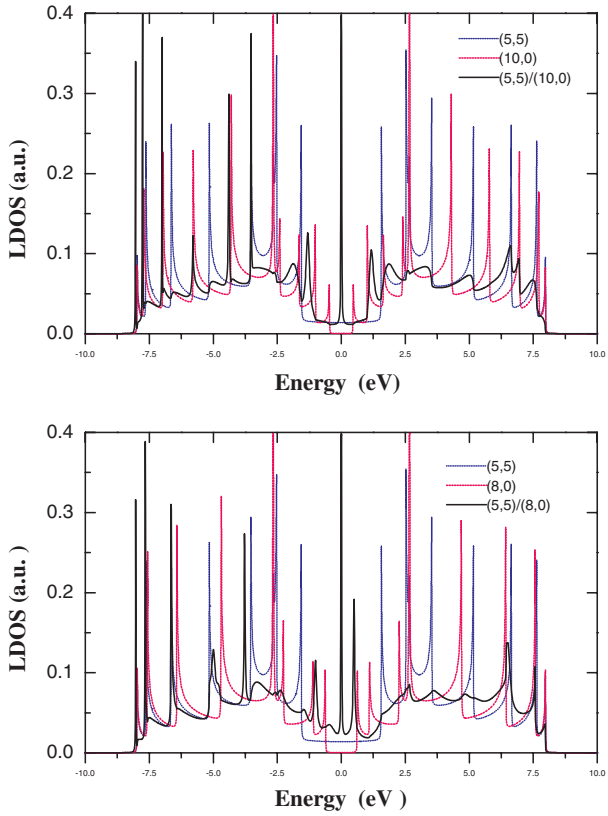

Fig. 3. Results for the S-M IMJs of (5,5)/(8,0) and (5,5)/(10,0), the results of constituent perfect tubes are also plotted for comparison.

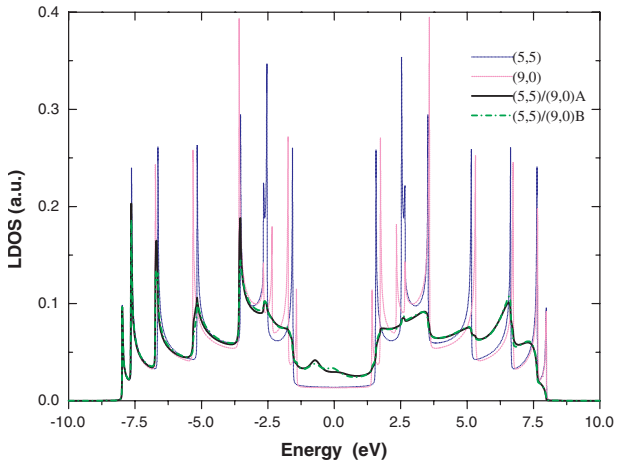

Fig. 4. Results for the M-M IMJs of (5,5)/(9,0)**A** and (5,5)/(9,0)**B**, the results of constituent perfect tubes are also plotted for comparison.

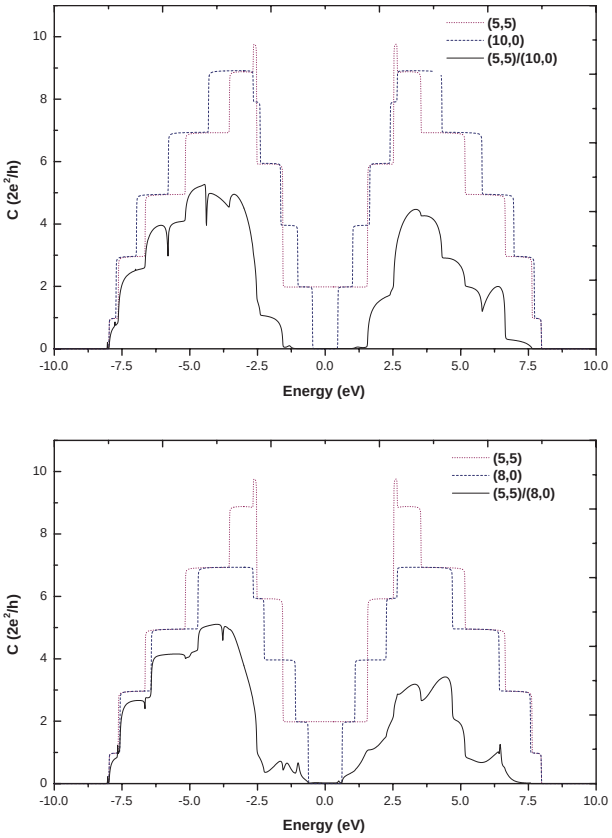

Fig. 5. Quantum conductances for the S-M IMJs of (5,5)/(8,0) and (5,5)/(10,0), the results of component perfect tubes are also plotted for comparison.

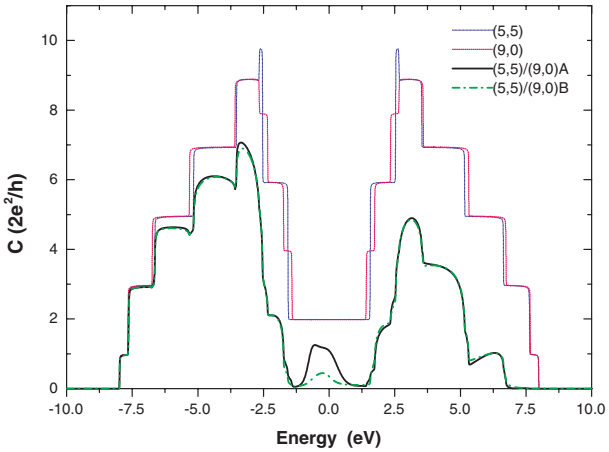

Fig. 6. Quantum conductances for the M-M IMJs of (5,5)/(9,0)**A** and (5,5)/(9,0)**B**, the results of component perfect tubes are also plotted for comparison.

S-M junctions. It corresponds to interface quasi-localized states, these discrete states can show Coulomb blockade, resonant transmission and energy quantization, which are desirable for the design for a quantum device [20]. This result is consistent with the previous predict [5], their calculations indicate the presence of a sharp MIG state in (5,5)/(10,0) M-S junction.

The transport properties through IMJs are illustrated in Figures 5 and 6, the quantum conductance of perfect constituent tubes are also plotted for comparison. Within the Landauer formalism, the ballistic conductance of perfect systems is proportional to the number of conducting channels at the Fermi energy, that is, the number of bands at this energy. All perfect metal tubes have two

bands at ϵ_F, giving rise to a conductance of $\frac{4e^2}{h}$ (Fig. 6). Whereas all semiconducting tubes have a gap at ϵ_F, hence the quantum conductance are zero (Fig. 5). The conductance of the matched tube is always smaller than the conductance of the perfect tubes that form it, and the suppression of the conductance to the conduction band is bigger than that of the valence band. Any defect degrades the conductance, and in a matched system A/B medium B can be considered as a perturbation to medium A and *vice versa*. For the presence of a vacancy in a monatomic chain completely suppresses the conductance by removing the only existing channel, since nanotube is a quasi-one-dimensional system and multichannel, the conductance is in general not totally suppressed; the extent to which it is depleted reflects the dimensionality [21]. Figure 5 shows that the conductance of M-S IMJs is still zero around Fermi energy ϵ_F though the allowed states appears in the energy gap around ϵ_F (see Figs. 3 and 5); Figure 6 shows the conductance of M-M IMJs along with the conductance of their perfect components, as before, the conductance of the matched tubes is lower at every energy than that of its perfect constituents. The decrease in conductance is accompanied by a small increase in the LDOS at the Fermi energy. This is due to the appearance of defect states associated with the pentagon-heptagon pairs within the metallic plateau near the Fermi level. These localized states behave as point scatterers in the electronic transmission process and are responsible for the decrease in conductance [22]. For the (5,5)/(9,0) M-M IMJ there exist two configurations **A** and **B**. It is very interesting that though the LDOS of the two configurations **A** and **B** of (5,5)/(9,0) look very similar, their conductance differ strongly as seen in Figure 6. The conductance of configuration **B** is much smaller than that of configurations **A** around the Fermi energy ϵ_F. The two matched tubes in general have different rotational symmetry about their cylindrical axes, and the electronic states may be classified according to discrete angular momenta L [21]. If the Fermi level states of the two perfect constituents have different L and the interface has common rotational symmetry with the constituents, the perfectly interface can't impart any extra angular momentum to the electron, so the conditions of energy and angular momentum conservation can't be satisfied simultaneously in the elastic scattering conduction process; the electron wave is totally reflected, and the conductance equals zero. For the two configurations **A** and **B** of (5,5)/(9,0) M-S junction, though the Fermi level states of the two constituents have different angular momentum **L**, since the interface of configuration **A** and **B** have no rotational symmetry, the interface can impart angular momentum to the electron, transitions through interface are permitted, this results in a nonzero conductance around Fermi energy ϵ_F; meanwhile the interface in configuration **A** is more irregular than that of configuration **B**, and can change the angular momentum **L** of the electron easier by scattering, so the conductance of configuration **A** is much larger. The above discussion about rotational symmetry has a meaning for non-chiral nanotubes only. As we have not changed the bonds strength at the matching region, this effect is attributed to the change in the lattice connectivity. That is, the conductance of two matched metallic SWNTs is very sensitive to their connectivity, certain configurations of the pentagon-heptagon pair defects completely stop the flow of electrons, while others permit the transmission of the current through the interface.

In summary, the electronic and transport properties of four different IMJs have been investigated by using the tight-binding-based Green's function method. Our results show that the structure defects can substantially modify the electronic and transport properties of SWNT. For the M-S IMJs, quasi-localized states can appear in the gap of its constituent semiconducting SWNT, which is desirable for the design for a quantum device; and the conductance of a M-M IMJ is very sensitive to its connectivity, certain configurations of connection completely stop the flow of electrons, while others permit the transmission of the current through the interface. These results may have implications for applications of present materials and aid in further developing our understanding of these molecular-scale structures.

References

1. G.Y. Tseng *et al.*, Science **294**, 1993 (2001)
2. S.J. Tans *et al.*, Nature (London) **393**, 49 (1998)
3. Y. Cui *et al.*, Science **291**, 851 (2001)
4. A. Bachtold *et al.*, Science **294**, 1317 (2001)
5. V. Derycke *et al.*, Nanolett. **1**, 453 (2001)
6. L. Chico *et al.*, Phys. Rev. Lett. **76**, 971 (1996)
7. R. Saito *et al.*, Phys. Rev. B **53**, 2044 (1996)
8. J.C. Charlier *et al.*, Phys. Rev. B **53**, 11108 (1996)
9. A. Rochefort, Ph. Avouris, Nanolett. **2**, 253 (2002)
10. J.W.G. Wildoeer *et al.*, Nature (London) **391**, 59 (1998); J.W. Odom *et al., ibid.* **391**, 62 (1998)
11. V. Meunier *et al.*, Phys. Rev. B **60**, 7792 (1999)
12. M. Ouyang *et al.*, Science **291**, 97 (2001)
13. M. Buongiorno Nardelli, Phys. Rev. B **60**, 7828 (1999)
14. M. Buongiorno Nardelli, J. Bernhoc, Phys. Rev. B **60**, R16338 (1999)
15. D.S. Fisher, P.A. Lee, Phys. Rev. B **23**, 6851 (1981)
16. Y. Meir, N.S. Wingreen, Phys. Rev. Lett. **68**, 2512 (1992)
17. S. Datta, *Electronic Transport in Mesoscopic Systems* (Cambridge University Press, Cambridge, 1995)
18. F. Garcia-Moliner *et al.*, Phys. Rep. **200**, 83 (1991)
19. M.P. Lopez-Sancho *et al.*, J. Phys. F **14**, 1205 (1984); *ibid.* **15**, 851 (1985)
20. L. Chico *et al.*, Phys. Rev. Lett. **81**, 1278 (1998)
21. L. Chico *et al.*, Phys. Rev. B **54**, 2600 (1996)
22. V.H. Crespi *et al.*, Phys. Rev. Lett. **79**, 2093 (1997)